

Molecular Cancer Therapeutics



The Novel VEGF Receptor/MET–Targeted Kinase Inhibitor TAS-115 Has Marked *In Vivo* Antitumor Properties and a Favorable Tolerability Profile

Hidenori Fujita, Kazutaka Miyadera, Masanori Kato, et al.

Mol Cancer Ther 2013;12:2685-2696. Published OnlineFirst October 18, 2013.

Updated version Access the most recent version of this article at:
doi:[10.1158/1535-7163.MCT-13-0459](https://doi.org/10.1158/1535-7163.MCT-13-0459)

Supplementary Material Access the most recent supplemental material at:
<http://mct.aacrjournals.org/content/suppl/2013/10/15/1535-7163.MCT-13-0459.DC1.html>

Cited Articles This article cites by 50 articles, 19 of which you can access for free at:
<http://mct.aacrjournals.org/content/12/12/2685.full.html#ref-list-1>

E-mail alerts [Sign up to receive free email-alerts](#) related to this article or journal.

Reprints and Subscriptions To order reprints of this article or to subscribe to the journal, contact the AACR Publications Department at pubs@aacr.org.

Permissions To request permission to re-use all or part of this article, contact the AACR Publications Department at permissions@aacr.org.

The Novel VEGF Receptor/MET-Targeted Kinase Inhibitor TAS-115 Has Marked *In Vivo* Antitumor Properties and a Favorable Tolerability Profile

Hidegori Fujita^{1,2}, Kazutaka Miyadera¹, Masanori Kato¹, Yayoi Fujioka¹, Hiroaki Ochiwa¹, Jinhong Huang¹, Kimihiro Ito¹, Yoshimi Aoyagi¹, Toru Takenaka¹, Takamasa Suzuki¹, Satoko Ito¹, Akihiro Hashimoto¹, Takashi Suefuji¹, Kosuke Egami¹, Hideki Kazuno¹, Yoshimitsu Suda¹, Kazuto Nishio², and Kazuhiko Yonekura¹

Abstract

VEGF receptor (VEGFR) signaling plays a key role in tumor angiogenesis. Although some VEGFR signal-targeted drugs have been approved for clinical use, their utility is limited by associated toxicities or resistance to such therapy. To overcome these limitations, we developed TAS-115, a novel VEGFR and hepatocyte growth factor receptor (MET)-targeted kinase inhibitor with an improved safety profile. TAS-115 inhibited the kinase activity of both VEGFR2 and MET and their signal-dependent cell growth as strongly as other known VEGFR or MET inhibitors. On the other hand, kinase selectivity of TAS-115 was more specific than that of sunitinib and TAS-115 produced relatively weak inhibition of growth ($GI_{50} > 10 \mu\text{mol/L}$) in VEGFR signal- or MET signal-independent cells. Furthermore, TAS-115 induced less damage in various normal cells than did other VEGFR inhibitors. These data suggest that TAS-115 is extremely selective and specific, at least *in vitro*. *In vivo* studies, TAS-115 completely suppressed the progression of MET-inactivated tumor by blocking angiogenesis without toxicity when given every day for 6 weeks, even at a serum-saturating dose of TAS-115. The marked selectivity of TAS-115 for kinases and targeted cells was associated with improved tolerability and contributed to the ability to sustain treatment without dose reduction or a washout period. Furthermore, TAS-115 induced marked tumor shrinkage and prolonged survival in MET-amplified human cancer-bearing mice. These data suggest that TAS-115 is a unique VEGFR/MET-targeted inhibitor with improved antitumor efficacy and decreased toxicity. *Mol Cancer Ther*; 12(12); 2685–96. ©2013 AACR.

Introduction

VEGF is a key factor involved in tumor vascularization (1). An association between the VEGF expression level and patient prognosis has been shown for many carcinomas (2–7). Bevacizumab, sunitinib, sorafenib, pazopanib, and axitinib are drugs that exert antitumor activities by inhibiting tumor vascularization through the suppression of VEGF function (8). Monotherapy with any of these drugs is effective against some carcinomas [e.g., gastrointestinal stromal tumor (GIST), renal cell carcinoma, hepatocellular carcinoma, and pancreatic neuroendocrine tumors], suggesting that the inhibition of the VEGF/VEGFR pathway is a valid strategy for the treatment of cancer. Neverthe-

less, these VEGFR-targeted inhibitor monotherapies for various other carcinomas, except for the abovementioned carcinomas, have only marginal effects, and none of these agents have adequate efficacy when used in combination with chemotherapeutic agents (9–13). One reason for this issue may be the unfavorable tolerability profile associated with these drugs, resulting in a high percentage of cases requiring dose reduction and/or treatment interruption. Therefore, this adverse tolerability profile prevents sufficient exposure otherwise needed to exert maximum effect by these drugs. In contrast, more tolerable drugs can be administered continuously for long treatment periods without the requirement for a washout period and are more likely to be able to be used in combination with conventional chemotherapeutic agents, thereby possibly improving their therapeutic efficacy.

MET, which serves as a receptor for hepatocyte growth factor (HGF), is a known proto-oncogene (14). The increased expression of HGF and the excessive expression of MET are reportedly involved in tumor progression (15), resistance to chemotherapeutic agents (16, 17), and are associated with poor outcomes in patients with solid cancers, such as gastric cancer (18), breast cancer (19), colorectal cancer (20), and lung cancer (21). The inhibition of the HGF/MET signal cascade can exert an antitumor

Authors' Affiliations: ¹Tsukuba Research Center, Taiho Pharmaceutical Co., Ltd., Tsukuba, Ibaraki; and ²Department of Genome Biology, Kinki University Faculty of Medicine, Osaka-Sayama, Osaka, Japan

Note: Supplementary data for this article are available at Molecular Cancer Therapeutics Online (<http://mct.aacrjournals.org>).

Corresponding Author: Hidegori Fujita, Tsukuba Research Center, Taiho Pharmaceutical Co., Ltd., 3 Okubo, Tsukuba, Ibaraki 300-2611, Japan. Phone: 81-29-865-4527; Fax: 81-29-865-2170; E-mail: hide-fujita@taiho.co.jp

doi: 10.1158/1535-7163.MCT-13-0459

©2013 American Association for Cancer Research.

effect in tumor cell lines with MET gene amplification, overexpression or overactivation (22, 23). In fact, numerous clinical trials examining the utility of MET inhibitors are now underway (24).

VEGFR and MET signaling pathways reportedly modulate tumor growth in a synergistic manner. Within tumor environments, HGF/MET signals and VEGF/VEGFR signals work in connection with: (i) the induction of VEGF expression by HGF/MET (25), (ii) the involvement of HGF/MET in the mechanism responsible for VEGFR inhibitor-resistant vascularization (26), (iii) the cooperation of HGF- and VEGF-induced vascularization (27), and so on. Therefore, dual inhibition of the VEGFR axis and the MET axis might exert synergistic antitumor activity due to blockade of the above pathways.

On the basis these observations, we attempted to develop a drug with a high inhibitory activity against the VEGFR and MET signal pathways and with improved safety profile. The present study describes the identification and characterization of TAS-115, a small-molecule inhibitor of VEGFR and MET, which was developed for this purpose.

Materials and Methods

Cell lines and cell cultures

The MKN45 and AZ-521 cell lines were obtained from Health Science Research Resources Bank (HSRRB; Tokyo, Japan). The MCF7, SK-OV-3, SK-BR-3, and normal diploid fibroblasts derived from fetal lung (MRC-5) cell lines were obtained from DS PharmaBiomedical. NUGC-4 was obtained from RIKEN Bio Resource Center. The DU145, HCT-116, and Hs746T cell lines were acquired from the

American Type Culture Collection (ATCC). The SC-9 cell line was provided by the Central Institute for Experimental Animals (Kawasaki, Japan). MS-1, a murine pancreatic islet endothelial cell line was purchased from ATCC. MKN45, NUGC-4, and SC-9 were human gastric carcinoma cell lines. MCF-7, SK-OV-3, HCT-116, and AZ-521 were human breast carcinoma, ovarian carcinoma, colorectal carcinoma, and duodenal carcinoma cell lines, respectively. Human umbilical vein endothelial cells (HUVEC), human coronary artery smooth muscle cells (hCASMC), and human alveolar epithelial cells (AEpiC) were obtained from Cell Systems, Inc., Cell Applications, Inc., and ScienCell Research Laboratories, respectively. Except for the SC-9 cells, all cell lines were cultured in the recommended media and serum concentrations, according to the instructions accompanying the cell lines. The SC-9 cell line was maintained by serial subcutaneous implantation (at 3-week intervals) into the right axillae of Balb/cnu/nu nude mice (Charles River Laboratories Japan, Inc.). We authenticated cancer cell lines by short tandem repeat inspection within 6 months after the end of these experiments. We provided same cryopreserved cell stock used in our experiments for short tandem repeat inspection. All cancer cell lines were identified. Normal cell lines were expended within 2 months from the beginning of culture after obtaining cell lines.

Reagents and antibodies

TAS-115 [4-[2-fluoro-4-[[[(2-phenylacetyl)amino]thioxomethyl]amino]-phenoxy]-7-methoxy-N-methyl-6-quinolinecarboxamide; Fig. 1A] was prepared by Taiho

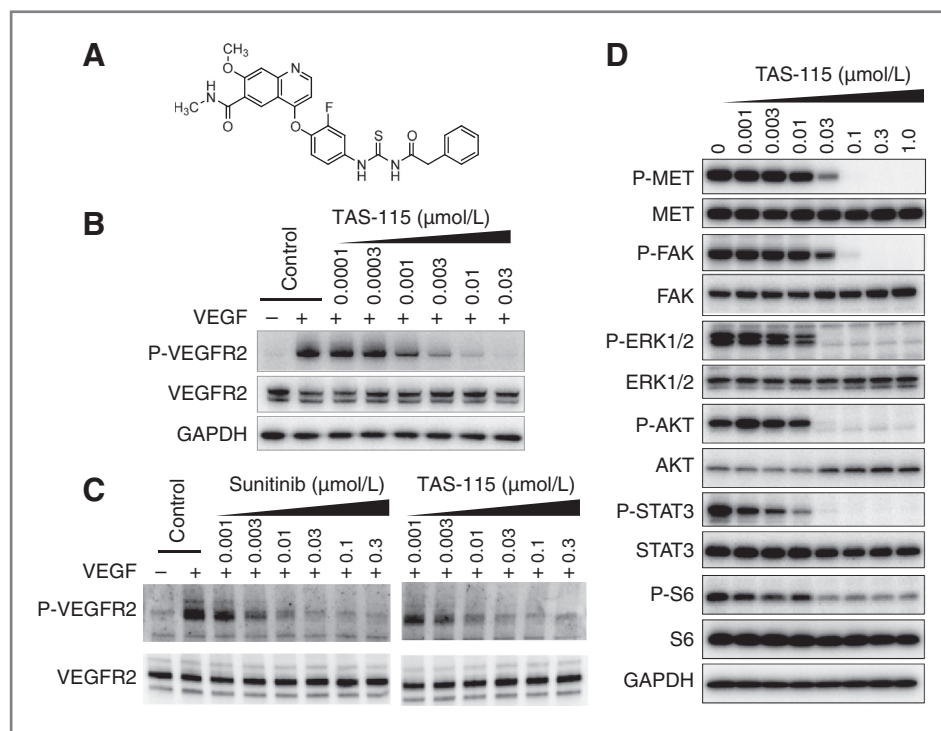


Figure 1. Cellular inhibition of the phosphorylation of VEGFR2, MET, and signaling factors downstream from MET by TAS-115. A, chemical structure of TAS-115. B, TAS-115-induced inhibition of VEGFR2 phosphorylation in VEGF-stimulated HUVECs. HUVECs were treated with the indicated concentrations of TAS-115 for 25 minutes. Then, VEGF (30 ng/mL) was added to the culture media. VEGF stimulation was performed for 5 minutes. C, TAS-115-induced inhibition of VEGFR2 phosphorylation in VEGF-stimulated MS-1 cells, which is a murine pancreatic islet endothelial cell line. D, TAS-115-induced inhibition of MET signal transduction in MKN45 cells. MKN45 cells, a MET-amplified human gastric cancer cell line, were treated with each of the indicated concentrations of TAS-115 for 30 minutes. "P-" indicates the phosphorylated form of each protein. GAPDH, glyceraldehyde 3-phosphate dehydrogenase

Pharmaceutical Co., Ltd.. Sorafenib and crizotinib were obtained from Chemrio International, Ltd. and Daicel Corporation, respectively. Sunitinib was synthesized in our laboratory according to published procedures (28).

Anti-MET antibody was acquired from Santa Cruz Biotechnology, Inc.. Anti-phosphorylated MET (Y1234/1235), anti-VEGFR, anti-phosphorylated VEGFR2 (Y1175), anti-phosphorylated extracellular signal-regulated kinase 1/2 (ERK 1/2; T202/Y204), anti-ERK 1/2, anti-phosphorylated AKT (S473), anti-AKT, anti-focal adhesion kinase (FAK), anti-S6, and anti-STAT3 antibodies were acquired from Cell Signaling Technology. Anti-glyceraldehyde 3-phosphate dehydrogenase (GAPDH) antibody was obtained from Trevigen, Inc.. Recombinant human VEGF and HGF were purchased from R&D Systems, Inc.. Anti-mouse CD31 antibody and anti-rat immunoglobulin G (IgG) conjugated with Alexa 568 were obtained from BD Pharmingen and Invitrogen Corporation, respectively. Anti-phosphorylated tyrosine antibody 4G10 was obtained from Millipore.

Kinase assays

Enzyme inhibition studies were performed using a mobility shift assay (29). Briefly, 0.3 $\mu\text{g}/\text{mL}$ of recombinant MET (rMET, N-terminal glutathione S-transferase (GST) Tag; Carna Biosciences) and 1.5 $\mu\text{mol}/\text{L}$ of FL-Peptide 2 (Caliper Life Sciences) or 2 $\mu\text{g}/\text{mL}$ of recombinant VEGFR2 (rVEGFR2, amino acid 790-end, N-terminal 6His Tagged; Upstate) and 1.5 $\mu\text{mol}/\text{L}$ of FL-Peptide 22 (Caliper Life Sciences) were added to a 25 μL mixture containing 1/2 the Michaelis constant (K_m) level of ATP, 100 mmol/L of HEPES (pH 7.2), 0.003% (w/v) Brij35, 0.04% (v/v) Tween 20, 10 mmol/L of MgCl_2 , 1 mmol/L of dithiothreitol, a Complete Mini EDTA-free Protease Inhibitor Cocktail Tablet (Roche Diagnostics, K.K.), and a PhosSTOP Phosphatase Inhibitor Cocktail Tablet (Roche Diagnostics, K.K.), with the addition of 0.05% (w/v) CHAPSO only in the case of rVEGFR2. The reaction mixture was incubated for 90 minutes at 28°C and was stopped by the addition of 15 mmol/L of EDTA. Phosphorylated peptide was calculated using a LabChip EZ Reader, Version 2.1.82.0 (UCC Version: 1.96, CCD Version: 102). On the basis of the amount of phosphorylated peptide formed in the control well and the drug-treated well, the 50% inhibitory concentration (IC_{50}) was calculated using a logistic regression analysis. A total of 192 kinase panel assays was performed using the ProfilerPro Kit 1-8 (Caliper Life Sciences) and was analyzed using a mobility shift assay.

Cellular MET and VEGFR2 phosphorylation assay

MKN45 cells were plated in 6-well plates. On the following day, TAS-115 was added to the wells at the desired final concentrations, and the cells were incubated for 30 minutes. After washing, the cells were lysed using Cell Extraction Buffer (Invitrogen Corporation). Cell lysate was analyzed using immunoblotting with the antibodies mentioned in the reagents and antibodies section.

To investigate cellular VEGFR2 phosphorylation, HUVECs were plated in collagen-coated dishes (BD Biosciences, Inc.). On the following day, serum starvation was performed during overnight incubation. Then, TAS-115 and VEGF were added at the desired final concentrations. After incubation for 5 minutes, cell lysate was prepared with Mammalian Protein Extraction Reagent (M-PER; Pierce Thermo Scientific) and VEGFR2 phosphorylation was detected using immunoblotting. Blotting images were analyzed using an LAS1000 plus with Multi Gauge, Ver. 3.0 (Fuji Photo Film). The relative signal value from the image was calculated using the signal intensity of GAPDH.

Quantification of cell proliferation and cell damage

Cancer cells were plated in a 96-well plate and allowed to adhere overnight. Then TAS-115 was added, followed by incubation for 72 hours. Cellular proliferation was evaluated using CellTiter-Glo (Promega Corp.). The drug-induced cell damage in normal cell lines was assessed using the signal of cell viability and caspase activity determined by crystal violet staining or the Apo-Tox-Glo Triplex Assay, and caspase 3/7 Glo (Promega Corp.), respectively. The drug-induced cell damage was evaluated using the signal derived from caspase 3/7 activity. The signal was normalized to cell viability. To investigate VEGF-dependent cell proliferation, HUVECs were cultured overnight under starvation conditions. Then, VEGF (30 ng/mL) and TAS-115 were added, followed by incubation for 24 hours. This assay was performed using the 5-bromo-2'-deoxyuridine uptake method (Roche).

In vivo efficacy studies

A SC-9 fragment was implanted subcutaneously into the right abdomen of each mouse via a trocar. Suspensions of MKN45 cells were prepared and were implanted subcutaneously into the right abdomen of each nude mouse. The tumor volume (TV, mm^3) was calculated as the length (mm) \times width (mm)²/2. The TAS-115 dose levels were set at 12.5, 50, and 200 $\text{mg}/\text{kg}/\text{d}$. The dose level for sunitinib was set at 40 $\text{mg}/\text{kg}/\text{d}$; this dose was equivalent to the maximum tolerated dose (MTD). Oral drug treatment was continued for 14 or 42 consecutive days for the chronic dosing in the SC-9 xenograft model. During the treatment period, TV and body weight were measured twice per week.

The antitumor efficacy was assessed at the end of each study period by calculating the tumor growth inhibition percentage (TGI; %). The TGI (%) values were calculated as $100 \times \{1 - [(TV_{\text{final}} - TV_{\text{initial}} \text{ for the treatment group})] / [(TV_{\text{final}} - TV_{\text{initial}} \text{ for the control group})] \}$. TV_{initial} and TV_{final} describe the tumor volumes on the allocation day and the final assessment day, respectively. When the TV_{final} was smaller than the TV_{initial} in the treatment group, tumor regression was judged to have occurred. The tumor regression values were determined by calculating the ratio of the mean TV_{initial} to the mean TV_{final} in

the treatment group. As an indicator of changes in body weight (BW) during the dosing period, the body weight change (BWC; %) was calculated as $100 \times [(BW \text{ on each measurement day}) - (BW_{\text{initial}})] / (BW_{\text{initial}})$. BW_{initial} describes the body weight on the allocation day.

Dunnett test was used as a statistical method to compare the tumor volume data in the drug-treated groups and the control group. Welch *t* test was used to compare the tumor volume in the TAS-115-treatment group with the highest efficacy and the comparative group. For all tests, $P < 0.05$ was used to indicate statistical significance.

For the peritoneal dissemination model, an NUGC-4 cell suspension (5×10^6 cells/mL) was prepared in 10% Matrigel (BD Biosciences, Inc.) and was inoculated intraperitoneally into nude mice. Sunitinib was administered once daily at 40 mg/kg, and TAS-115 was administered once daily at 50 or 200 mg/kg for 5 days each week. The increased life span (ILS) was calculated using the median survival time (MST) in each treatment group. The mice were euthanized by isoflurane inhalation upon becoming moribund. The survival times of the drug treatment groups and the control group were compared using a log-rank test. $P < 0.05$ was regarded as being statistically significant.

All animal experiments were conducted in accordance with the guidelines for animal experiments at Taiho Pharmaceutical Co., Ltd.

Measurement of tumor vascular density

SC-9 tumor-bearing nude mice were orally treated with TAS-115 for 4 consecutive days, and the tumor was removed on day 5. Frozen sections were prepared and exposed to a biotin-conjugated anti-mouse CD31 antibody. Then, the sections were stained using the Metal Enhanced DAB Substrate Kit (Pierce Thermo Scientific). Pictures were taken of eight visual fields/section within each stained section, i.e., four lateral fields and four medial fields of the tumor. The tumor vessel density (TVD, No. of tumor vessels/mm²) was calculated using the equation given below:

$$\text{TVD} = (\text{total number of vessels in 8 visual fields}) / (\text{area of one visual field} \times 8)$$

To detect the tumor vessels by fluorescent immunohistochemistry, the tumor sections were immunolabeled with anti-mouse CD31 antibody and stained with anti-rat IgG conjugated Alexa 568. The stained sections were then assessed under a fluorescent microscope (AXIO Imager A1; Carl Zeiss).

Pharmacodynamic studies using tumor xenografts

To perform VEGFR2 pharmacodynamic analysis, AZ-521 tumor-bearing nude mice were orally treated with TAS-115. Three hours after TAS-115 treatment, VEGF was injected via the caudal vein at a dose of 10 µg/body. The tumor was removed from each mouse at 5 minutes after the injection of VEGF. Then, the tumor lysate was prepared using a lysis buffer [200 mmol/L Tris-HCl (pH 7.5), 100 mmol/L NaCl, 20 mmol/L EDTA, 1% Triton X-100] for immunoprecipitation with anti-VEGFR2 antibody (R&D Systems, Inc.). VEGFR2 and its phosphorylated form were detected using immunoblotting with an anti-VEGFR2 antibody and an anti-phosphorylated tyrosine antibody 4G10.

MET pharmacodynamics analysis was investigated in MKN45 tumor-bearing nude mice. Three hours after TAS-115 treatment, the tumor was removed and lysed using Cell Extraction Buffer (Invitrogen Corporation). MET, ERK1/2, AKT, and their phosphorylated forms were detected using immunoblotting with the abovementioned antibodies.

Results

TAS-115 potently inhibited the catalytic activity of VEGFR2 and MET kinase

The ability of TAS-115 to inhibit VEGFR2 and MET as well as the manner of the inhibition were analyzed. The IC₅₀ values of TAS-115 against rVEGFR2 and rMET were 0.030 and 0.032 µmol/L, respectively (Table 1). The manner of kinase inhibition by TAS-115 was shown to be ATP antagonism with inhibition constant (K_i) values against rVEGFR2 and rMET of 0.012 and 0.039 µmol/L, respectively. In our assay system, the IC₅₀ values of sunitinib and sorafenib against rVEGFR2 were 0.018 and 0.072 µmol/L, respectively, and the IC₅₀ value of crizotinib against rMET was 0.016 µmol/L. Thus, the inhibitory activity of TAS-115 against rVEGFR2 and rMET was approximately equal to that of the other examined VEGFR- or MET-targeted kinase inhibitors.

Kinase selectivity of TAS-115 was investigated using a 192-kinase panel assay. The IC₅₀ of TAS-115 was less than 1 µmol/L for 53 (28%) of 192 kinases. These data revealed TAS-115 also inhibited platelet-derived growth factor receptor-α and -β (PDGFRs), AXL receptor tyrosine kinase (AXL), c-kit receptor tyrosine kinase (KIT), sarcoma virus tyrosine kinase (SRC), and fms-like tyrosine kinase-1 (FLT-1) kinase activity. The IC₅₀ of sunitinib

Table 1. Kinase inhibitory activity of TAS-115 for recombinant VEGFR2 and MET in a kinase assay

Kinase	IC ₅₀ (mean ± SD; µmol/L)			
	TAS-115	Sunitinib	Sorafenib	Crizotinib
VEGFR2	0.030 ± 0.009	0.018 ± 0.004	0.073 ± 0.019	>3.0
MET	0.032 ± 0.014	>3.0	>3.0	0.016 ± 0.009

was less than 1 $\mu\text{mol/L}$ for 82 (43%) kinases and the kinase inhibitory spectrum of sunitinib was broad (Supplementary Table S1). These data demonstrated that the action of TAS-115 was more selective when compared with sunitinib.

TAS-115 inhibited cellular phosphorylation in VEGF-stimulated endothelial cells and MET-amplified cancer cells

Chemical structure of TAS-115 was described in Fig. 1A. In VEGF-stimulated HUVECs, TAS-115 markedly inhibited the tyrosine phosphorylation of VEGFR2 at more than 0.01 $\mu\text{mol/L}$ (Fig. 1B). TAS-115 also inhibited cellular phosphorylation of VEGFR2 in MS-1 cells at concentrations indicating phospho-VEGFR2 inhibition in HUVECs (Fig. 1C). These data reveal that there was no difference in cellular VEGFR2 inhibition by TAS-115 when comparing human and murine cells. MKN45 cells, a MET gene-amplified human gastric cancer cell line, demonstrate increased phosphorylation of MET. TAS-115 markedly inhibited the tyrosine phosphorylation of MET in MKN45 cells (Fig. 1D). TAS-115 also markedly inhibited the phosphorylation of ERK 1/2, AKT, FAK, S6, and STAT3 (all of which are signal transduction factors located downstream from MET) at a concentration of more than 0.03 $\mu\text{mol/L}$ (Fig. 1D). These results indicate that TAS-115 suppresses signal transduction in the mitogen-activated protein kinase (MAPK) and phosphoinositide 3-kinase (PI3K)/AKT pathways by inhibiting MET in MET-amplified cancer cells. Thus, TAS-115 inhibited the phosphorylation

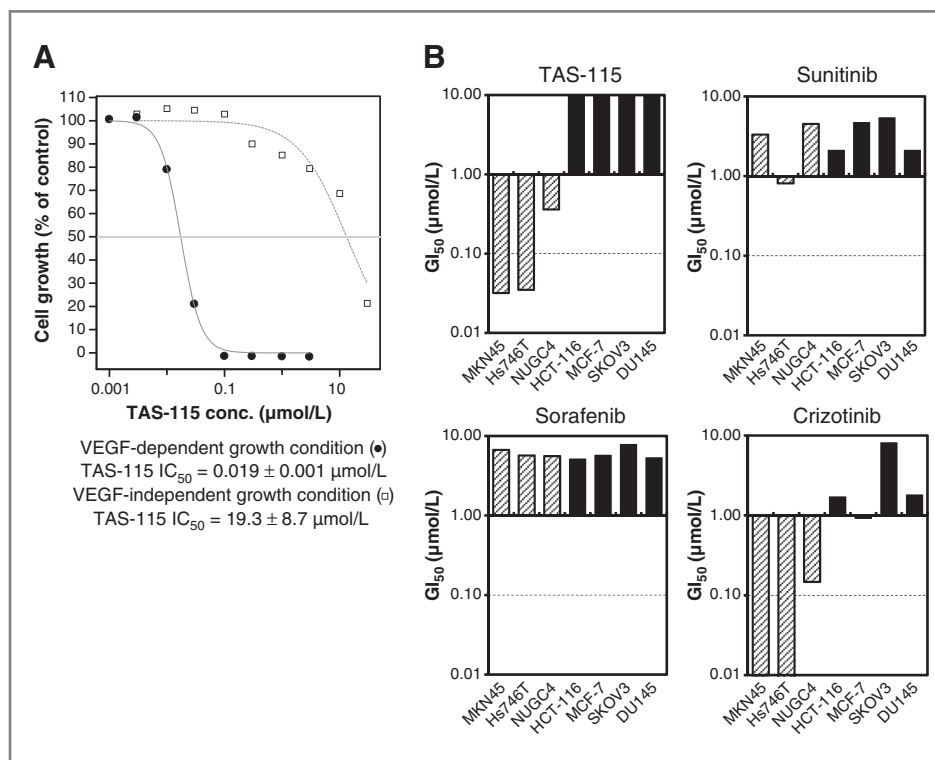
of cellular VEGFR2 and MET at concentrations similar to those capable of inhibiting rVEGFR2 and rMET.

TAS-115 inhibits VEGF- or MET-dependent cell growth in a highly selective manner

The effect of TAS-115 against VEGF-dependent endothelial cell proliferation was investigated in HUVECs. TAS-115 strongly inhibited the cellular proliferation of HUVECs under VEGF-dependent growth condition with an IC_{50} value of 0.019 $\mu\text{mol/L}$ (Fig. 2A). Meanwhile, the inhibitory activity of TAS-115 against cellular proliferation under VEGF-independent growth conditions using media containing 10% FBS was very weak ($\text{IC}_{50} = 19 \mu\text{mol/L}$, Fig. 2A).

Because TAS-115 also inhibited the activity of MET kinase, it markedly suppressed proliferation of MKN45, Hs746T, and NUGC-4 cells (MET-amplified cancer cell lines). The 50% growth inhibitory concentration (GI_{50}) value of TAS-115 against MKN45, Hs746T, and NUGC-4 cells was 0.032, 0.035, and 0.362 $\mu\text{mol/L}$, respectively (Fig. 2B). While TAS-115 inhibited growth of these MET-amplified cancer cell lines, it did not lead to cell death in these cell lines, even when used at concentrations of 3 $\mu\text{mol/L}$ (Supplementary Fig. S1). In addition, TAS-115 produced less growth inhibition against MET-inactivated cancer cells with a GI_{50} value of more than 10 $\mu\text{mol/L}$ (Fig. 2B; Supplementary Table S2). Sunitinib and sorafenib uniformly inhibited the growth of all examined cancer cell lines with a GI_{50} value of less than 10 $\mu\text{mol/L}$ (Fig. 2B; Supplementary Table S2). These data indicate

Figure 2. TAS-115-induced highly potent and selective inhibition of MET and VEGFR signal-dependent cell growth. **A**, inhibitory activities of TAS-115 against the VEGF-dependent or -independent proliferation of HUVECs. Cell growth ratio (%) in TAS-115-treated versus control in the VEGF-dependent condition (●) and in the VEGF-independent condition (□). The VEGF-independent condition consisted of 10% FBS without the addition of VEGF. **B**, selective inhibition of TAS-115 against MET-amplified cancer cell proliferation. MKN45, Hs746T, and NUGC-4 were the MET-amplified cancer cell lines. HCT-116, MCF-7, SK-OV-3, and DU145 showed no MET amplification. The 50% growth inhibitory concentration (GI_{50}) values are presented as the mean value of three independent tests.



that TAS-115 inhibited proliferation of VEGF-dependent endothelial cells and MET-amplified cancer cells in a highly selective manner when compared with other VEGFR or MET inhibitors.

TAS-115 causes minimal damage to normal cells

We investigated the effect of TAS-115 on various normal cell lines, including rat cardiomyocytes (Fig. 3A), hCASM (Fig. 3B), MRC5 (Fig. 3C), and AEpiC (Fig. 3D). Caspase activity in each cell line after treatment was measured as an indicator of apoptosis and was normalized to cell viability. TAS-115 treatment produced minimal caspase activity in normal cell lines, even at a TAS-115 concentration of 10 $\mu\text{mol/L}$. In contrast, sunitinib, sorafenib, and crizotinib treatment resulted in significantly increased caspase activity in these normal cell lines. In rat cardiomyocytes, although caspase induction by sunitinib or sorafenib was moderate at 72 hours after treatment (Fig. 3A), sunitinib or sorafenib-induced caspase activity was markedly enhanced at 96 hours after treatment (Supplementary Fig. S2). TAS-115 did not increase caspase activ-

ity in rat cardiomyocytes even after 96 hours. These results suggested that the toxicity profile of TAS-115 in normal cells is less than that of other VEGFR-targeted kinase inhibitors.

Uninterrupted inhibition of angiogenesis by VEGFR-targeted kinase inhibitor is required to significantly inhibit tumor growth.

To verify the antitumor efficacy of TAS-115 as a VEGFR inhibitor with consecutive dosing, chronological changes in tumor progression were investigated. TAS-115 dose-dependently inhibited phosphorylation of VEGFR2 and angiogenesis in tumors after 4 consecutive days of treatment, and the antiangiogenesis potency at TAS-115 200 mg/kg was comparable with that of sunitinib (Fig. 4A and B). Consecutive dosing at 200 mg/kg/d of TAS-115 completely prevented tumor growth during the treatment period, with no body weight loss observed in animals with SC-9 xenografts, even at TAS-115 dosing of 200 mg/kg/d (Fig. 4C). Of note, the body weight of mice in the TAS-115 treatment group gradually increased, while that in the

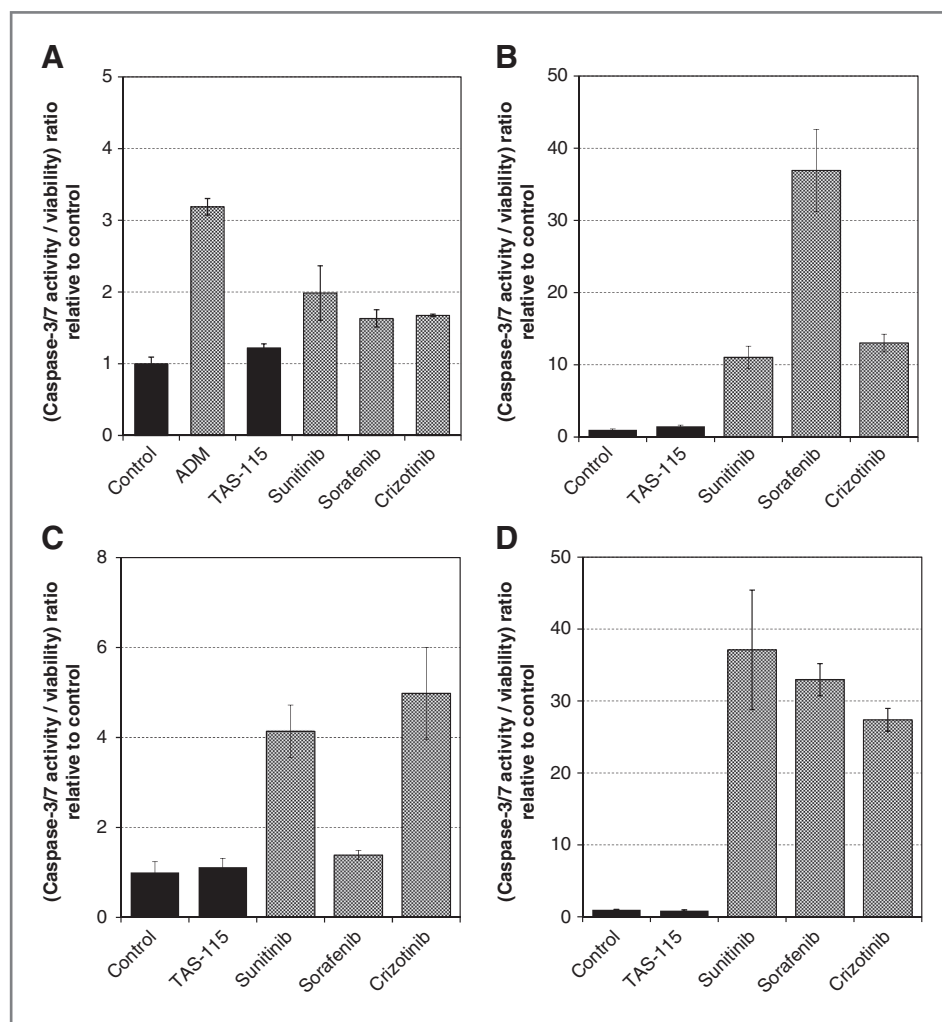


Figure 3. Kinase inhibitor-induced cell damage in normal cells. Rat cardiomyocytes (A), human coronary artery smooth muscle cells (hCASM; B), normal diploid fibroblast derived from fetal lung (MRC5; C) and human alveolar epithelial cells (AEpiC; D) were plated and cultured in TAS-115-, sunitinib-, sorafenib- and crizotinib-containing medium for 72 hours. Cell viability was evaluated using crystal violet staining or the ApoTox-Glo Triplex Assay (Promega Corp.). Each caspase 3/7 activation level was normalized with cell viability. A, adriamycin (ADM) was added at 1 $\mu\text{mol/L}$. TAS-115 and other drugs were added at 10 $\mu\text{mol/L}$. B, TAS-115 and other drugs were added at 10 $\mu\text{mol/L}$. C, TAS-115 and sorafenib were added at 10 $\mu\text{mol/L}$. Sunitinib and crizotinib were added at 5 $\mu\text{mol/L}$, because cell viability was not observed at 10 $\mu\text{mol/L}$. D, sorafenib was added at 3.3 $\mu\text{mol/L}$ because of severe toxicity. Other drug concentrations were 10 $\mu\text{mol/L}$.

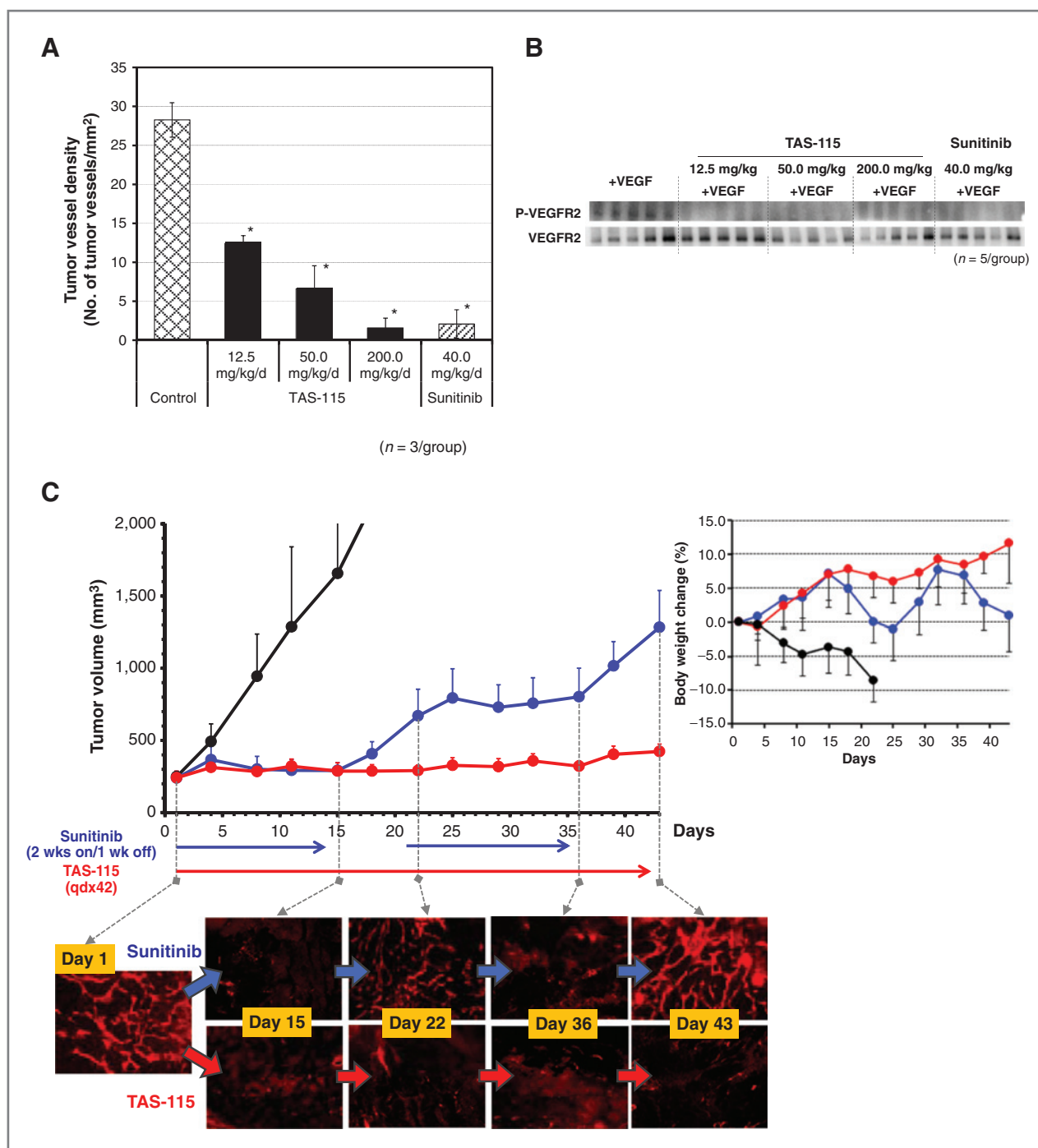


Figure 4. Chronic treatment with TAS-115 produced potent antitumor effects by inhibiting angiogenesis. **A**, tumor vessel density in SC-9 xenografts after TAS-115 or sunitinib treatment for 4 consecutive days. Each bar indicates the SD. *, $P < 0.05$ in the treated group according to a Dunnett test, when compared with the control group. **B**, TAS-115–induced inhibition of VEGFR2 phosphorylation in tumor xenografts. VEGF was administered intravenously to athymic mice bearing human duodenal carcinoma AZ-521 xenografts at 3 hours after TAS-115 treatment. Five minutes later, the tumor was removed from each mouse and prepared for immunoblotting. "P-" indicates the phosphorylated form of VEGFR. **C**, antitumor effect of consecutive TAS-115 treatment in gastric carcinoma SC-9 xenografts expressing low levels of MET, and staining of tumor vessels at each of the indicated time points. SC-9 tumor-bearing athymic mice were treated with TAS-115 (200 mg/kg/d; 42 consecutive days) or sunitinib (40 mg/kg/d; 2 weeks on/1 week off $\times 2$ to mimic a clinical regimen). Each plotted dot indicates the mean tumor volume, and each bar indicates the SD ($n = 6$ /group). Treatment was initiated when the mean tumor volume was approximately 250 mm³. The tumors were harvested before drug administration (day 1) and before and after the drug-off period of sunitinib treatment (days 15, 22, 36, and 43). These samples were examined using immunofluorescence staining of the tumor vessels with anti-mouse CD31 antibody ($n = 3$ /time point). Right graph shows body weight change (%) in this study from day 1 during the TAS-115 treatment period. Mice in the control group were euthanized at day 22 because of tumor ulceration.

vehicle-treated (control) group decreased. Furthermore, TAS-115 markedly suppressed tumor vascular development over a 42-day treatment period (Fig. 4C). Sunitinib was administered with 2-weeks-on/1-week-off regimen in 3-week cycles to mimic clinical regimens incorporating a washout period. Consecutive dosing of sunitinib for 14 days also completely blocked tumor growth and tumor angiogenesis; however, rapid tumor regrowth and tumor blood vessels remodeling were observed at 7 days after treatment suspension (Fig. 4C). Surprisingly, after a sunitinib washout period of only 7 days, the tumor blood vessels returned to the number and phenotype similar to that seen before sunitinib treatment, and tumors ultimately showed regrowth. Gene expression analysis of *Flt-1*, *Flk-1*, *Pecam-1* and *Tie-2* was also examined in SC-9 tumor tissues after TAS-115 or sunitinib treatment (Supplementary Fig. S3). Changes in expression of these genes were considered as indicators of endothelial cells contents in tumor tissue, because these genes are mainly expressed in endothelial cells. In the sunitinib-treated group, expression of all four genes was lower at day 15 when compared with day 1 (pretreatment). However, the gene expression at day 43 was similar to that at day 1. Changes in gene expression seemed to coincide with blood vessel changes demonstrated by immunohistochemistry. In the TAS-115-treated group, expression of all 4 genes was suppressed at day 15 and day 43 when compared with that at day 1. Thus, consecutive dosing without drug withdrawal is important to maintain the optimal therapeutic effect of a VEGFR-targeted kinase inhibitor.

Antitumor efficacy of TAS-115 in MET-amplified human cancer transplanted models

We evaluated the antitumor efficacy of TAS-115 against MET-amplified human cancer implanted models. When MKN45 tumor-bearing nude mice were orally treated with TAS-115 for 14 consecutive days, the TGI value was 76% at a dose of 12.5 mg/kg/d (Fig. 5A; $P < 0.001$). TAS-115 at a dose of 50 mg/kg/d completely prevented tumor growth during the treatment period. TAS-115 at a dose of 200 mg/kg/d induced a 48% regression from the initial tumor volume (Fig. 5B). The estimated 50% effective dose (ED_{50} ; the dose at which the TGI value was 50%) of TAS-115 in this model was 8 mg/kg/d. Sunitinib also produced significant tumor growth inhibition (TGI = 84%; $P < 0.001$) but did not induce tumor regression in this xenograft model (Fig. 5A and B). TAS-115 markedly inhibited the phosphorylation of MET and signal transduction factors located downstream from MET (i.e., ERK and AKT) at a dose of 3.1 mg/kg (Fig. 5C). In the other MET-amplified cancer cell lines, TAS-115 induced tumor regression, and the estimated ED_{50} for these tumors was roughly 2 to 8 mg/kg/d, based on the relationship between the dose and the TGI values (Supplementary Fig. S4).

To more clearly evaluate the potent efficacy and safety of TAS-115, the survival benefit of TAS-115 was investigated using an NUGC-4 peritoneal metastasis model. NUGC-4 is a MET-amplified human gastric carcinoma

cell line (30). The MST from the day of implantation in the control group and sunitinib treatment group was 29 and 23 days, respectively. The MST in the TAS-115 treatment groups was 41 and more than 60 days at a dose of 50 and 200 mg/kg/d, respectively. TAS-115 significantly prolonged the survival period of the NUGC-4 peritoneal metastasis model mice ($P < 0.01$), while sunitinib did not ($P = 0.119$) (Fig. 5D). The ILS in the TAS-115 treatment group was 41% and more than 100% at doses of 50 and 200 mg/kg/d, respectively (Supplementary Table S3). TAS-115 significantly prolonged survival of these mice when administered at doses of 50 or 200 mg/kg/d ($P < 0.001$, log-rank test).

These results demonstrate that the dual inhibition of VEGFR and MET was more effective against MET-amplified tumors than VEGFR inhibition alone. Furthermore, the efficacy and safety of this regimen allowed chronic treatment, which was associated with further improvements in outcomes.

Discussion

VEGF/VEGFR signaling is essential for intratumoral vascularization and is involved in tumor progression. Some approved VEGFR-targeted inhibitors are effective for GIST, renal cell carcinoma, hepatocellular carcinoma, and pancreatic neuroendocrine tumors, but the efficacy of these agents for other kinds of carcinoma or when used in combination with chemotherapies is not favorable. An improvement in the associated tolerability profile as well as the antitumor efficacy is critical to overcoming these limitations. MET is involved primarily in tumor growth, invasion, metastasis, and angiogenesis (31). These insights suggest that the combination of MET inhibition and VEGFR inhibition might enhance the anti-tumor efficacy of VEGFR-targeted inhibitors.

We recently discovered a highly potent compound, TAS-115, that was capable of inhibiting both MET and VEGFR2 via ATP antagonism. The IC_{50} of TAS-115 against VEGFR2 and MET was 0.030 and 0.032 $\mu\text{mol/L}$, respectively, indicating that the inhibitory activity of TAS-115 against VEGFR2 and MET is comparable with that of other VEGFR- or MET-targeted kinase inhibitor (e.g., sunitinib, sorafenib, and crizotinib). Kinase selectivity of TAS-115 was also evaluated using a 192-kinase panel assay (Supplementary Table S1). The IC_{50} of TAS-115 was less than 1 $\mu\text{mol/L}$ for 53 (28%) of 192 kinases, whereas the IC_{50} of sunitinib was less than 1 $\mu\text{mol/L}$ for 82 (43%) kinases. These data suggest that TAS-115 is more selective than sunitinib and, therefore, has less off-target effects.

TAS-115 was shown to powerfully suppress the VEGF-dependent proliferation of HUVECs ($IC_{50} = 0.019 \mu\text{mol/L}$) as a VEGFR-targeted inhibitor and powerfully suppress the proliferation of MET-amplified cancer cells ($GI_{50} = 0.032\text{--}0.362 \mu\text{mol/L}$) as a MET-targeted inhibitor. However, TAS-115 did not induce cell death in the examined MET-amplified cancer cell lines (Supplementary Fig. S1). In addition, it had a markedly lower effect on VEGFR or MET signal-independent cell proliferation ($GI_{50} > 10$

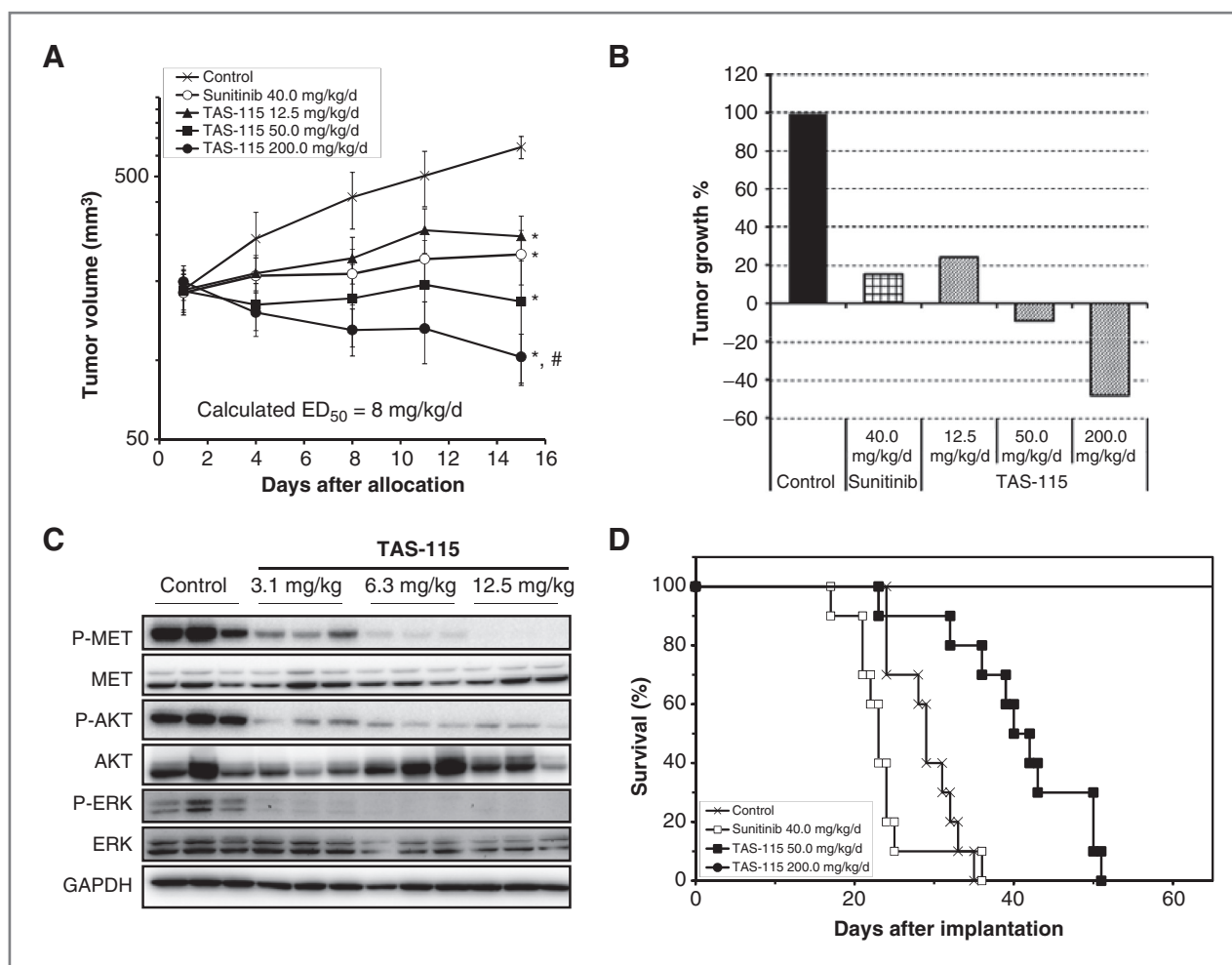


Figure 5. Antitumor efficacy of TAS-115 against MET-amplified human gastric cancer MKN45 xenograft models. **A**, TAS-115–induced time-dependent tumor volumes changes of human gastric carcinoma MKN45 xenografts. TAS-115 and sunitinib were orally administered consecutively from day 1 to day 14. Each plotted dot indicates the mean tumor volume, and each bar indicates the standard deviation. *, $P < 0.05$ in the treated group according to Dunnett's test when compared with the control. #, $P < 0.05$ in the TAS-115 (200 mg/kg/d)-treated group according to Welch t test when compared with the sunitinib-treated group. **B**, tumor growth (%) in each treatment group on day 15. The tumor volume difference between day 1 and day 15 was set as 100% growth. Tumor growth (%) was calculated using the tumor volume difference in each group when compared with the control. Tumor regression from day 1 was described below 0 (%). **C**, inhibition of MET signal transduction by TAS-115 treatment in human gastric carcinoma MKN45 xenografts. Three hours after administration of the indicated dose of TAS-115, the tumor in each mouse was removed and prepared for immunoblotting. **D**, Kaplan–Meier curves for an NUGC-4 peritoneal dissemination model. Each treatment group contained 10 mice.

μmol/L) when compared with other VEGFR-targeted kinase inhibitors. Furthermore, TAS-115 produced only minimal damage to normal cell lines, even when used at a concentration of 10 μmol/L. In contrast, other VEGFR- or MET-targeted kinase inhibitors produced significant cell damage in various normal cell lines, including rat cardiomyocytes, when used at concentrations comparable with those used for TAS-115. During clinical development, VEGFR-targeted inhibitors were recognized to cause cardiovascular toxicity (32), possibly via reduction of nitric oxide function in endothelial cells (33) and due to capillary rarefaction based on VEGF/VEGFR signal inhibition (34). Other mechanisms by which multi-kinase inhibition can produce cardiotoxicity have been described (35). For example, sunitinib inhibits adenosine monophosphate

(AMP)-activated protein kinase (AMPK), which plays a key role as a master regulator of cellular energy homeostasis, resulting in damage to cardiomyocytes (36). We confirmed that sunitinib inhibited kinase activity of AMPK-α with an IC₅₀ value of 0.061 μmol/L and that sunitinib suppressed cellular phosphorylation and activity of AMPK-α in rat cardiomyocytes at 1 μmol/L (Supplementary Fig. S5). Meanwhile, TAS-115 did not inhibit kinase activity or cellular phosphorylation of AMPK-α in rat cardiomyocytes even at 10 μmol/L. In this study, AMPK inhibition by sunitinib resulted in damage to rat cardiomyocytes. In addition to AMPK inhibition, a multi-kinase inhibitor, such as sunitinib, might induce non-specific cellular damage via its off-target action. The present study showed that TAS-115 had much less toxicity in

various normal cell lines when compared with other VEGFR-targeted kinase inhibitors.

In an *in vivo* antitumor efficacy study, TAS-115 could be administered consecutively at a high dose, such as saturating drug concentration in blood, and therefore exerted potent antitumor activity via antiangiogenesis against human gastric cancer SC-9 xenografts. Sunitinib also strongly suppressed tumor growth for 14 consecutive days in this model. However, during each sunitinib washout period or after sunitinib withdrawal, tumors showed rapid regrowth. Similar observations have been noted in clinical practice when using VEGFR-targeted kinase inhibitors (37, 38). The mechanisms mediating "withdrawal flare" are not understood, but modulation of plasma levels of circulating proteins involved in VEGF signaling during VEGFR inhibitor treatment might lead to tumor progression. These observations suggest that VEGFR-targeted kinase inhibitors should be administered without interruption and dose reduction in order to be effective. The selectivity of TAS-115 allowed for chronic dosing and improved tolerability, thereby enhancing the overall efficacy of this regimen and obviating the risk of withdrawal flare.

TAS-115 also demonstrated prominent MET inhibition and suppressed MET-amplified cancer cell proliferation *in vitro*. Moreover, TAS-115 induced tumor shrinkage and prolonged survival in MET-amplified human cancer transplanted models. The antitumor activity of TAS-115 against MET-amplified human gastric cancer MKN45 xenografts was higher than those of sunitinib. Although TAS-115 did not cause marked cell death in MKN45, even when used at a concentration of 3 $\mu\text{mol/L}$, the *in vitro* proliferation assay showed that TAS-115 induced marked tumor regression when used at 200 mg/kg/d in MKN45 xenograft models. Similar results were also observed in experiments using other MET-amplified cancer cell lines (Supplementary Figs. S1 and S4). The mechanism of action of TAS-115-induced tumor regression in MET-amplified human cancer xenografts is not known at present. Considering that sunitinib, a VEGFR-targeted multi-kinase inhibitor, could not produce tumor regression in MKN45 xenograft models, TAS-115-induced tumor regression may be derived from inhibition of both VEGFR and MET in this specific tumor microenvironment. Indeed, synergistic action between VEGFR and MET signaling in tumor progression has been previously described. HGF/MET signaling also plays a role as a proangiogenesis factor in endothelial cells independent of VEGF/VEGFR signaling (26, 27). Furthermore, HGF upregulates VEGF expression and downregulates thrombospondin-1 in cancer cells (25, 39). The HGF-mediated change in the expression of these factors promotes tumor angiogenesis. These insights might explain the action of HGF/MET signaling as an endogenous resistance factor for VEGFR-targeted inhibitors (40, 41). Furthermore, HGF/MET signaling activity is greater under hypoxic conditions after VEGFR-targeted inhibitors treatment than under normoxia, and hypoxia-induced HGF/MET signaling activity may reinforce tumor progression and metastasis (42). The abovementioned

insights suggest that VEGFR and MET signaling act in concert to promote tumor growth. Thus, simultaneous inhibition of VEGFR and MET might exert greater antitumor efficacy when compared with inhibition of either element alone.

The estimated ED₅₀ values for several MET-amplified tumor xenograft models in this study were 2–8 mg/kg/d. MET-induced signal transduction in tumors was obviously inhibited after TAS-115 treatment at the ED₅₀. Because the MTD of TAS-115 was more than 200 mg/kg/d, the safety margin calculated by the ED₅₀ and the MTD was more than 25-fold. This suggests that TAS-115 is highly potent and has a favorable safety profile *in vivo* (43). In the human gastric cancer NUGC-4 peritoneal metastasis model, chronic treatment with TAS-115 improved survival and did not have any severe toxic effects.

The balance between efficacy and safety must be optimized to improve the therapeutic efficacy of molecularly targeted drugs. During clinical studies, the percentage of patients requiring a dose reduction of these molecularly targeted drugs is relatively high (44, 45), and the outcome of treatment with these drugs has not been satisfactory, even when they have been used in combination with other anticancer agents (46–49). The requirement for a washout period and/or dose reduction when using presently available VEGFR inhibitors may result in tumor regrowth and drug resistance (50).

In summary, treatment with TAS-115 produced relatively selective dual inhibition of VEGFR and MET and resulted in marked antitumor effects. Furthermore, the increased tolerability of this regimen allowed chronic treatment with this drug, thereby further enhancing overall efficacy. The improved tolerability profile of this agent may allow its coadministration with other chemotherapeutic agents, possibly leading to further improvements in outcomes.

Disclosure of Potential Conflicts of Interest

No potential conflicts of interest were disclosed.

Authors' Contributions

Conception and design: H. Fujita, K. Miyadera, Y. Suda, K. Nishio, K. Yonekura

Development of methodology: J. Huang, Y. Aoyagi

Acquisition of data (provided animals, acquired and managed patients, provided facilities, etc.): H. Fujita, M. Kato, Y. Fujioka, H. Ochiwa, J. Huang, K. Ito, T. Takenaka, T. Suzuki, S. Ito, A. Hashimoto, H. Kazuno

Analysis and interpretation of data (e.g., statistical analysis, biostatistics, computational analysis): J. Huang, K. Ito

Writing, review, and/or revision of the manuscript: H. Fujita, Y. Suda, K. Nishio, K. Yonekura

Administrative, technical, or material support (i.e., reporting or organizing data, constructing databases): K. Miyadera, K. Ito, T. Suefuji, K. Egami

Study supervision: K. Miyadera, K. Yonekura

Grant Support

This study was supported by Taiho Pharmaceutical Co., Ltd.

The costs of publication of this article were defrayed in part by the payment of page charges. This article must therefore be hereby marked *advertisement* in accordance with 18 U.S.C. Section 1734 solely to indicate this fact.

Received June 7, 2013; revised September 12, 2013; accepted September 26, 2013; published OnlineFirst October 18, 2013.

References

- Hicklin DJ, Ellis LM. Role of the vascular endothelial growth factor pathway in tumor growth and angiogenesis. *J Clin Oncol* 2005;23:1011-27.
- Gasparini G, Toi M, Gion M, Verderio P, Dittadi R, Hanatani M, et al. Prognostic significance of vascular endothelial growth factor protein in node-negative breast carcinoma. *J Natl Cancer Inst* 1997;89:139-47.
- Maeda K, Chung YS, Ogawa Y, Takatsuka S, Kang SM, Ogawa M, et al. Prognostic value of vascular endothelial growth factor expression in gastric carcinoma. *Cancer* 1996;77:858-63.
- Kang SM, Maeda K, Onoda N, Chung YS, Nakata B, Nishiguchi Y, et al. Combined analysis of p53 and vascular endothelial growth factor expression in colorectal carcinoma for determination of tumor vascularity and liver metastasis. *Int J Cancer* 1997;74:502-7.
- Jantus-Lewintre E, Sanmartin E, Sirera R, Blasco A, Sanchez JJ, Taron M, et al. Combined VEGF-A and VEGFR-2 concentrations in plasma: diagnostic and prognostic implications in patients with advanced NSCLC. *Lung Cancer* 2011;74:326-31.
- Schoenleber SJ, Kurtz DM, Talwalkar JA, Roberts LR, Gores GJ. Prognostic role of vascular endothelial growth factor in hepatocellular carcinoma: systematic review and meta-analysis. *Br J Cancer* 2009;100:1385-92.
- Jacobsen J, Rasmuson T, Grankvist K, Ljungberg B. Vascular endothelial growth factor as prognostic factor in renal cell carcinoma. *J Urol* 2000;163:343-7.
- Tugues S, Koch S, Gualandi L, Li X, Claesson-Welsh L. Vascular endothelial growth factors and receptors: anti-angiogenic therapy in the treatment of cancer. *Mol Aspects Med* 2011;32:88-111.
- Bergh J, Bondarenko IM, Lichinitser MR, Liljegren A, Greil R, Voytko NL, et al. First-line treatment of advanced breast cancer with sunitinib in combination with docetaxel versus docetaxel alone: results of a prospective, randomized phase III study. *J Clin Oncol* 2012;30:921-9.
- Scagliotti G, Novello S, von Pawel J, Reck M, Pereira JR, Thomas M, et al. Phase III study of carboplatin and paclitaxel alone or with sorafenib in advanced non-small-cell lung cancer. *J Clin Oncol* 2010;28:1835-42.
- Teoh D, Secord AA. Antiangiogenic agents in combination with chemotherapy for the treatment of epithelial ovarian cancer. *Int J Gynecol Cancer* 2012;22:348-59.
- Rugo HS, Stopeck AT, Joy AA, Chan S, Verma S, Lluch A, et al. Randomized, placebo-controlled, double-blind, phase II study of axitinib plus docetaxel versus docetaxel plus placebo in patients with metastatic breast cancer. *J Clin Oncol* 2011;29:2459-65.
- Ocana A, Amir E, Vera F, Eisenhauer EA, Tannock IF. Addition of bevacizumab to chemotherapy for treatment of solid tumors: similar results but different conclusions. *J Clin Oncol* 2011;29:254-6.
- Bottaro DP, Rubin JS, Falletto DL, Chan AM, Kmiecik TE, Vande Woude GF, et al. Identification of the hepatocyte growth factor receptor as the c-met proto-oncogene product. *Science* 1991;251:802-4.
- Birchmeier C, Birchmeier W, Gherardi E, Vande Woude GF. Met, metastasis, motility and more. *Nat Rev Mol Cell Biol* 2003;4:915-25.
- Bowers DC, Fan S, Walter KA, Abounader R, Williams JA, Rosen EM, et al. Scatter factor/hepatocyte growth factor protects against cytotoxic death in human glioblastoma via phosphatidylinositol 3-kinase- and AKT-dependent pathways. *Cancer Res* 2000;60:4277-83.
- Fan S, Wang JA, Yuan RQ, Rockwell S, Andres J, Zlatapolskiy A, et al. Scatter factor protects epithelial and carcinoma cells against apoptosis induced by DNA-damaging agents. *Oncogene* 1998;17:131-41.
- Lee J, Seo JW, Jun HJ, Ki CS, Park SH, Park YS, et al. Impact of MET amplification on gastric cancer: possible roles as a novel prognostic marker and a potential therapeutic target. *Oncol Rep* 2011;25:1517-24.
- Lengyel E, Prechtel D, Resau JH, Gauger K, Welk A, Lindemann K, et al. C-Met overexpression in node-positive breast cancer identifies patients with poor clinical outcome independent of Her2/neu. *Int J Cancer* 2005;113:678-82.
- Kammula US, Kuntz EJ, Francone TD, Zeng Z, Shia J, Landmann RG, et al. Molecular co-expression of the c-Met oncogene and hepatocyte growth factor in primary colon cancer predicts tumor stage and clinical outcome. *Cancer Lett* 2007;248:219-28.
- Masuya D, Huang C, Liu D, Nakashima T, Kameyama K, Haba R, et al. The tumour-stromal interaction between intratumoral c-Met and stromal hepatocyte growth factor associated with tumour growth and prognosis in non-small-cell lung cancer patients. *Br J Cancer* 2004;90:1555-62.
- Jin H, Yang R, Zheng Z, Romero M, Ross J, Bou-Reslan H, et al. MetMab, the one-armed 5D5 anti-c-Met antibody, inhibits orthotopic pancreatic tumor growth and improves survival. *Cancer Res* 2008;68:4360-8.
- Mayor S. MET inhibitors: translating from bench to bedside. *Lancet Oncol* 2011;12:14.
- Peters S, Adjei AA. MET: a promising anticancer therapeutic target. *Nat Rev Clin Oncol* 2012;9:314-26.
- Zhang YW, Su Y, Volpert OV, Vande Woude GF. Hepatocyte growth factor/scatter factor mediates angiogenesis through positive VEGF and negative thrombospondin 1 regulation. *Proc Natl Acad Sci U S A* 2003;100:12718-23.
- Shojaei F, Lee JH, Simmons BH, Wong A, Esparza CO, Plumlee PA, et al. HGF/c-Met acts as an alternative angiogenic pathway in sunitinib-resistant tumors. *Cancer Res* 2010;70:10090-100.
- Sulpice E, Ding S, Muscatelli-Groux B, Berge M, Han ZC, Plouet J, et al. Cross-talk between the VEGF-A and HGF signalling pathways in endothelial cells. *Biol Cell* 2009;101:525-39.
- Sun L, Liang C, Shirazian S, Zhou Y, Miller T, Cui J, et al. Discovery of 5-[5-fluoro-2-oxo-1,2-dihydroindol-(3Z)-ylidenemethyl]-2,4-dimethyl-1H-pyrrole-3-carboxylic acid (2-diethylaminoethyl)amide, a novel tyrosine kinase inhibitor targeting vascular endothelial and platelet-derived growth factor receptor tyrosine kinase. *J Med Chem* 2003;46:1116-9.
- Card A, Caldwell C, Min H, Lokchander B, Hualin X, Sciabola S, et al. High-throughput biochemical kinase selectivity assays: panel development and screening applications. *J Biomol Screen* 2009;14:31-42.
- Asaoka Y, Tada M, Ikenoue T, Seto M, Imai M, Miyabayashi K, et al. Gastric cancer cell line Hs746T harbors a splice site mutation of c-Met causing juxtamembrane domain deletion. *Biochem Biophys Res Commun* 2010;394:1042-6.
- Gherardi E, Birchmeier W, Birchmeier C, Vande Woude G. Targeting MET in cancer: rationale and progress. *Nat Rev Cancer* 2012;12:89-103.
- Chu TF, Rupnick MA, Kerkela R, Dallabrida SM, Zurawski D, Nguyen L, et al. Cardiotoxicity associated with tyrosine kinase inhibitor sunitinib. *Lancet* 2007;370:2011-9.
- Facemire CS, Nixon AB, Griffiths R, Hurwitz H, Coffman TM. Vascular endothelial growth factor receptor 2 controls blood pressure by regulating nitric oxide synthase expression. *Hypertension* 2009;54:652-8.
- Vaklavas C, Lenihan D, Kurzrock R, Tsimberidou AM. Anti-vascular endothelial growth factor therapies and cardiovascular toxicity: what are the important clinical markers to target? *Oncologist* 2010;15:130-41.
- Schmidinger M, Zielinski CC, Vogl UM, Bojic A, Bojic M, Schukro C, et al. Cardiac toxicity of sunitinib and sorafenib in patients with metastatic renal cell carcinoma. *J Clin Oncol* 2008;26:5204-12.
- Kerkela R, Woulfe KC, Durand JB, Vagnozzi R, Kramer D, Chu TF, et al. Sunitinib-induced cardiotoxicity is mediated by off-target inhibition of AMP-activated protein kinase. *Clin Transl Sci* 2009;2:15-25.
- Liu G, Jeraj R, Vanderhoek M, Perlman S, Kolesar J, Harrison M, et al. Pharmacodynamic study using FLT PET/CT in patients with renal cell cancer and other solid malignancies treated with sunitinib malate. *Clin Cancer Res* 2011;17:7634-44.
- Desar IM, Mulder SF, Stillebroer AB, van Spronsen DJ, van der Graaf WT, Mulders PF, et al. The reverse side of the victory: flare up of symptoms after discontinuation of sunitinib or sorafenib in renal cell cancer patients. A report of three cases. *Acta Oncol* 2009;48:927-31.
- Matsumura A, Kubota T, Taiyoh H, Fujiwara H, Okamoto K, Ichikawa D, et al. HGF regulates VEGF expression via the c-Met receptor

- downstream pathways, PI3K/Akt, MAPK and STAT3, in CT26 murine cells. *Int J Oncol* 2013;42:535–42.
40. Jahangiri A, De Lay M, Miller LM, Carbonell WS, Hu YL, Lu K, et al. Gene expression profile identifies tyrosine kinase c-Met as a targetable mediator of anti-angiogenic therapy resistance. *Clin Cancer Res* 2013;19:1773–83.
 41. Tran HT, Liu Y, Zurita AJ, Lin Y, Baker-Neblett KL, Martin AM, et al. Prognostic or predictive plasma cytokines and angiogenic factors for patients treated with pazopanib for metastatic renal-cell cancer: a retrospective analysis of phase 2 and phase 3 trials. *Lancet Oncol* 2012;13:827–37.
 42. Shojaei F, Simmons BH, Lee JH, Lappin PB, Christensen JG. HGF/c-Met pathway is one of the mediators of sunitinib-induced tumor cell type-dependent metastasis. *Cancer Lett* 2012;320:48–55.
 43. Ochiwa H, Fujita H, Ito K, Takenaka T, Huang J, Ito S, et al. The prominent safety profile of TAS-115, a novel c-Met + VEGFR dual kinase inhibitor can lead to potentiate the efficacy via durable inhibition of angiogenesis. *Cancer Res* 71:8s, 2011 (suppl; abstr 3600).
 44. van der Veldt AA, Boven E, Helgason HH, van Wouwe M, Berkhof J, de Gast G, et al. Predictive factors for severe toxicity of sunitinib in unselected patients with advanced renal cell cancer. *Br J Cancer* 2008;99:259–65.
 45. Cohen RB, Oudard S. Antiangiogenic therapy for advanced renal cell carcinoma: management of treatment-related toxicities. *Invest New Drugs* 2012;30:2066–79.
 46. Carrato A, Swieboda-Sadlej A, Staszewska-Skurczynska M, Lim R, Roman L, Shparyk Y, et al. Fluorouracil, leucovorin, and irinotecan plus either sunitinib or placebo in metastatic colorectal cancer: a randomized, phase III trial. *J Clin Oncol* 2013;31:1341–7.
 47. Scagliotti GV, Krzakowski M, Szczesna A, Strausz J, Makhson A, Reck M, et al. Sunitinib plus erlotinib versus placebo plus erlotinib in patients with previously treated advanced non-small-cell lung cancer: a phase III trial. *J Clin Oncol* 2012;30:2070–8.
 48. Gradishar WJ, Kaklamani V, Sahoo TP, Lokanatha D, Raina V, Bondarde S, et al. A double-blind, randomised, placebo-controlled, phase 2b study evaluating sorafenib in combination with paclitaxel as a first-line therapy in patients with HER2-negative advanced breast cancer. *Eur J Cancer* 2013;49:312–22.
 49. Goncalves A, Gilibert M, Francois E, Dahan L, Perrier H, Lamy R, et al. BAYPAN study: a double-blind phase III randomized trial comparing gemcitabine plus sorafenib and gemcitabine plus placebo in patients with advanced pancreatic cancer. *Ann Oncol* 2012;23:2799–805.
 50. Mancuso MR, Davis R, Norberg SM, O'Brien S, Sennino B, Nakahara T, et al. Rapid vascular regrowth in tumors after reversal of VEGF inhibition. *J Clin Invest* 2006;116:2610–21.